Contract No:

This document was prepared in conjunction with work accomplished under Contract No. 89303321CEM000080 with the U.S. Department of Energy (DOE) Office of Environmental Management (EM).

Fused Filament Fabrication of Polycarbonate in a Reactive Atmosphere

Seth Hall

Abstract. Fused Filament Fabrication (FFF) has become extremely useful in various industries, particularly when complex parts are needed in low volumes. However, the material properties available in FFF polymers are limited in scope. The properties of a FFF part can be changed in multiple ways. This study explores changing the bulk properties of a part by affecting each layer as it prints. Prior work has demonstrated the feasibility of altering polymer properties by layerwise exposure to a liquid chemical, but properties have never been modified in situ using a reactive gas. Here, FFF is done in the presence of a reactive gas. Specifically, the part is printed with polycarbonate in a reactive atmosphere of ozone and ultra-violet light. It was found that as each layer is exposed to a reactive gas, the bulk properties of the part change. A visual chemical change was seen, as well as confirmation of the reaction through Fourier transform infrared spectroscopy attenuated total reflectance. The change in mechanical properties was measured through Dynamic Mechanical Analysis shear tests, showing a bulk change can be efficiently produced through FFF in a reactive atmosphere.

I. INTRODUCTION

Additive manufacturing (AM) or 3D printing is a relatively new manufacturing technique yet has grown rapidly in use. AM can be used to manufacture parts with geometries that are impossible or difficult to make with standard manufacturing techniques. An advantage to AM is the ability to make many different parts without needing custom molds or special tooling for each part. This allows a wide array of parts to be made in areas with limited space.[1-3]

However, a drawback of AM is mechanical weakness resulting from weak interlayer adhesion. This creates inherent anisotropic properties in the part.[4, 5] This issue has been studied with fused filament fabrication (FFF), as it is one of the most common methods of AM.[5] This method deposits a heated polymer layer by layer until the part is created. Research by Perryman and Dadmun showed that the interlayer adhesion can be increased by spraying a reactive liquid on each layer.[6] This strengthening decreased with the amount of time taken to print each layer. As larger and more complicated parts are made, it would be beneficial to remove that extra manufacturing step and the dependence on time.

This study explores the possibility of printing in a reactive gas environment. In such an environment, each layer is exposed to a reactive gas as it is being printed. This removes the added time needed to spray the surface with a liquid reactant.

The candidate reaction chosen for testing was polycarbonate with ozone and ultra-violet (UV) light. Polycarbonate was chosen as it is known to show evidence of a reaction after only ten seconds at room temperature with ozone and UV.[7-10] In FFF, the thermoplastic layer cools rapidly after being deposited onto the part. This leaves only 2-5 seconds where the temperature is above the glass transition temperature, where reaction kinetics are more favorable.[11] Other polymers, such as polylactic acid, were considered but disregarded as the reaction would occur too slowly on the timescale of printing. Bhurke, et al. found that the reaction with polycarbonate and ozone creates changes in adhesion, wettability, and other mechanical surface properties.[8] Changes in the surface of the polymer were seen through a decrease in water contact angle and increased surface cross-linking.[8] These changes in surface properties can change bulk properties when used in conjunction with additive manufacturing, as each layer in the part is a surface that is exposed to the reaction.

II. Methods

A. Printer Setup

As seen in Figure 1, the Ultimaker 2+ printer is placed inside an environment-controlled chamber, specifically the Purair P5-48XT. Two VMUS-4 ozone generators feed ozone in through a tube that is directly connected to the extrusion nozzle, shown in Figure 2. This is to ensure ozone concentration is as high as possible around the nozzle to facilitate as many reactions as possible within each layer. Each generator fluctuates between 3 and 3.2 SLPM, leading to a total of 6 to 6.4 SLPM of ozone pumped into the chamber. Two UV lamps are placed above the printer, with a total lamp power at the surface measured to be ~4.8mw/cm. The wavelength of light is centered at 365 nm. The use of two UV lamps is to ensure that the reacting polycarbonate is exposed to UV light on the whole surface. The samples are printed at 5 mm/s, slower than maximum operating speed, to allow time for the reaction to progress. The print bed of the chamber has a temperature of 110°C, while the nozzle temperature is at 260°C. The size and shape of the sample that is printed depends on the test being performed on that sample. For example, for shear testing, small cylinders are made, but for tensile tests, dog bone specimens are made.

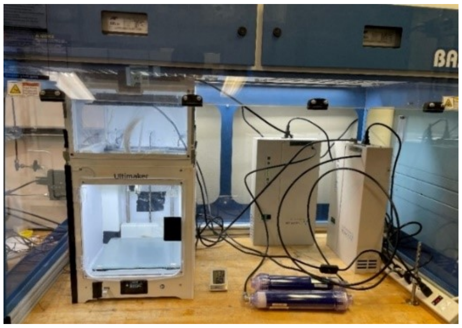

Figure 1: The printer next to the two ozone generators. The ozone generators are connected to dehumidifiers to reduce the amount of water in the system.

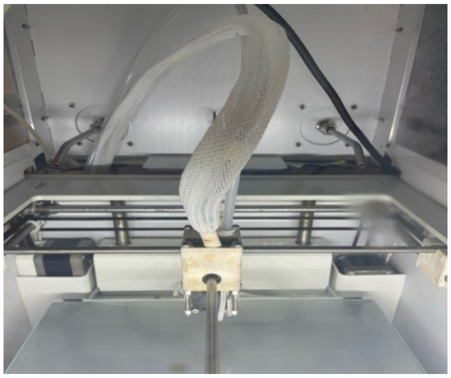

Figure 2: A top-down view of the print bed. The filament is fed through the back, while ozone comes in through the tube in the front.

B. Filament Production

The PcMAX polycarbonate pellets used were bought from 3DXTECH. These pellets were dried in an oven overnight at 65°C with desiccant. The pellets were dried to remove any water, as water on the pellets will create bubbles in the filament. The pellets were then fed into the Filabot EX2 Extruder filament making machine, shown in Figure 3. The polycarbonate is then extruded along the Filabot Airpath, a series of fans to cool it, then fed through a measuring device (Filameasure) and put into a spool (Filabot Spooler). The average filament diameter extruded was 2 mm. The filament was extruded at 245 °C at 80 % of the Filabot's maximum screw speed. This filament was then used in the printer to produce both the control samples and the reacted samples.

Figure 3: The Filabot EX2 Extruder (left), the Filabot airpath (middle) and the Fialabot Spooler (right).

C. Fourier transform infrared spectroscopy (FTIR)

Fourier transform infrared spectroscopy attenuated total reflectance (FTIR-ATR) was used to measure the infrared absorption spectra of both the treated and untreated printed samples. This was done to identify any chemical changes in the material after printing under ozone and UV conditions. This measurement was done on the top surface of the printed part. The machine used was the JASCO 6300. 32 scans were averaged for each sample. The data was baseline corrected at 4000 cm^{-1} and peak normalized at 1505 cm^{-1}.

D. Dynamic Mechanical Analysis (DMA)

Dynamic mechanical analysis is another method used to characterize materials. It is especially useful in understanding the viscoelastic behavior of polymers. The instrument used was the Mettler Toledo DMA/SDTA 1+. It was used in shear stress testing mode to observe the stiffness of the samples. Four conditions were run, printing in air with and without UV light, and printing in ozone with and without UV light. At least three trials in each condition were run. The samples were printed to be cylinders with a diameter of 8 mm and a height of 2 mm. To test shear stress, two identically sized samples are placed in the assembly. The frequency tested was 1 Hz. Force and displacement were measured from 30 to 200 °C. This in turn allows storage modulus, loss modulus, and tan(δ) to be calculated.

E. Differential Scanning Calorimetry (DSC)

Differential scanning calorimetry (DSC) measures heat flow across a sample. This is useful in identifying certain material properties, such as the glass transition temperature or the melting behavior. Each sample was cut to fit in an aluminum 40 µL pan. The samples were 6.37 mg with a standard deviation of 0.89 mg. The method used was a heat-cool-heat procedure from -30 to 250 °C at 10 °C/min

III. Sample Testing and Analysis

A. Visual

The first indication that a chemical change occurred throughout the material is a distinct color change in the samples that were printed in conditions with ozone and UV light. To demonstrate this color change, Figure 4 shows four samples printed in each condition. Similarly, three "Benchy" models were printed, shown in Figure 5. Benchy is a 3D model that includes many of the benchmarks of AM including overhanging and complicated shapes.[14] The first (Figure 5a) was printed in air without UV light. The second (Figure 5b) was printed halfway with the ozone and UV light on, then was turned off and printed the rest of the way in air. Figure 5c was printed under UV light and ozone the entire print. As the color change only occurs under ozone exposure, it is assumed that some chemical reaction is occurring. More quantitative evidence of the reaction will be discussed in the next section.

Figure 4: Four cylindrical sample prints. From left to right, they were printed in air, in air with UV light, in ozone, and in ozone with UV light. A distinct color change is seen in those exposed to ozone.

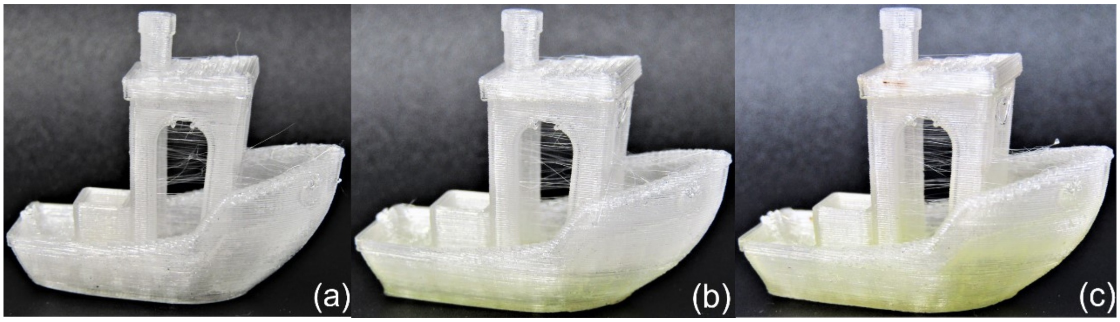

Figure 5: Three different Benchy prints. The first was printed in air, the second with ozone/UV turned on midway through the print, and the third with ozone/UV on the whole time. There is a distinct color change to the areas printed in ozone with UV light.

B. FTIR-ATR

Transmittance was measured from 4000-400 cm^{-1} as shown in Figure 6c. Two regions of interest are highlighted. Across three different samples, a consistent reduction in the peak is seen just below 3000 cm^{-1}, indicative of a change in the alkane C-H stretching. This is shown in Figure 6a. There is also a broadening of the peak just below 1800 cm^{-1}, indicative of a change in the C=O stretching[12] (shown in Figure 6b). This indicates that those functional groups of the polymer have been changed in some way, as a change in peak width indicates bonding with a different chemical environment than seen in the samples that were printed in air. Verkuijlen et al. showed an FTIR-ATR spectra of polycarbonate reacted with ozone with noticeable peaks around 1650 and 3500 cm^{-1}.[12] There are two reasons that might explain why this data does not show similar results. First, the polycarbonate used in this study was printed in air that was dehumidified. Second, the reaction in this study occurred at printing temperatures of 260 °C, causing different reaction kinetics.

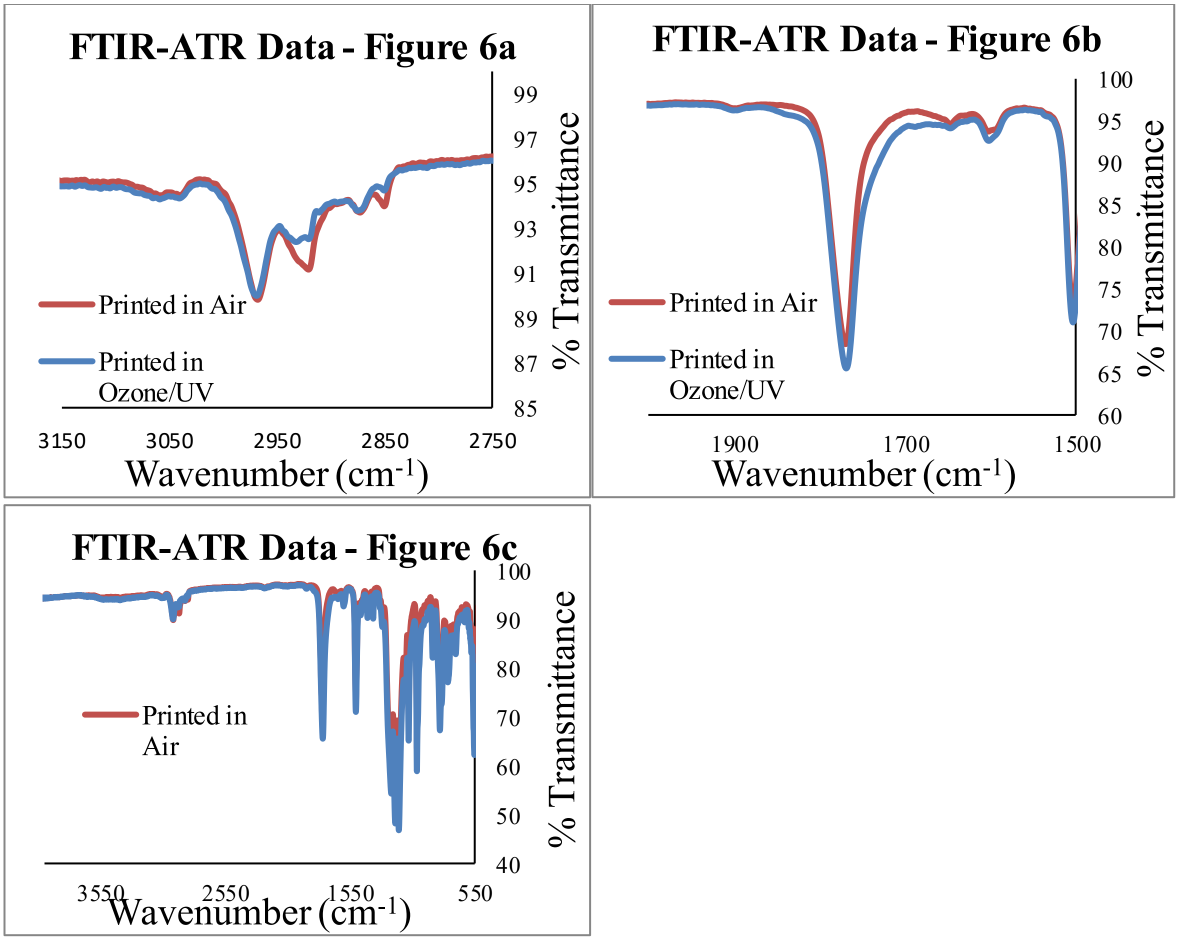

Figure 6: The two regions of interest shown in figures "6a" and "6b", with the full spectrum shown in "6c".

C. DMA

Significant changes in each trial were noticed by graphing tan(δ), which is the ratio of storage modulus to loss modulus (Figure 7). The peak of tan(δ) is taken to be the glass transition temperature. All measured glass transition temperatures are shown in Table 1, showing no statistical difference under each printing condition. However, there is a consistent broadening of the base of the tan(δ) peak under both printing conditions exposed to ozone, with the one exposed to UV light having the broadest base. A larger peak width can contribute to either higher polydispersity or evidence of two peaks.[2-3] If there were an increase in polydispersity, no chemical change would be present. However, as seen in the FTIR in the previous section, a chemical change is seen. This leads to the conclusion that there are two glass transition temperatures and two materials present.

Printing Conditions	Glass Transition (°C)	Standard Dev. (°C)
Air, No UV	153.9	0.0
Air, UV	154.0	0.5
O3, No UV	154.0	0.2
O3, UV	153.9	0.1

Table 1: The tan(δ) peak showed no statistically significant difference in the glass transition temperature.

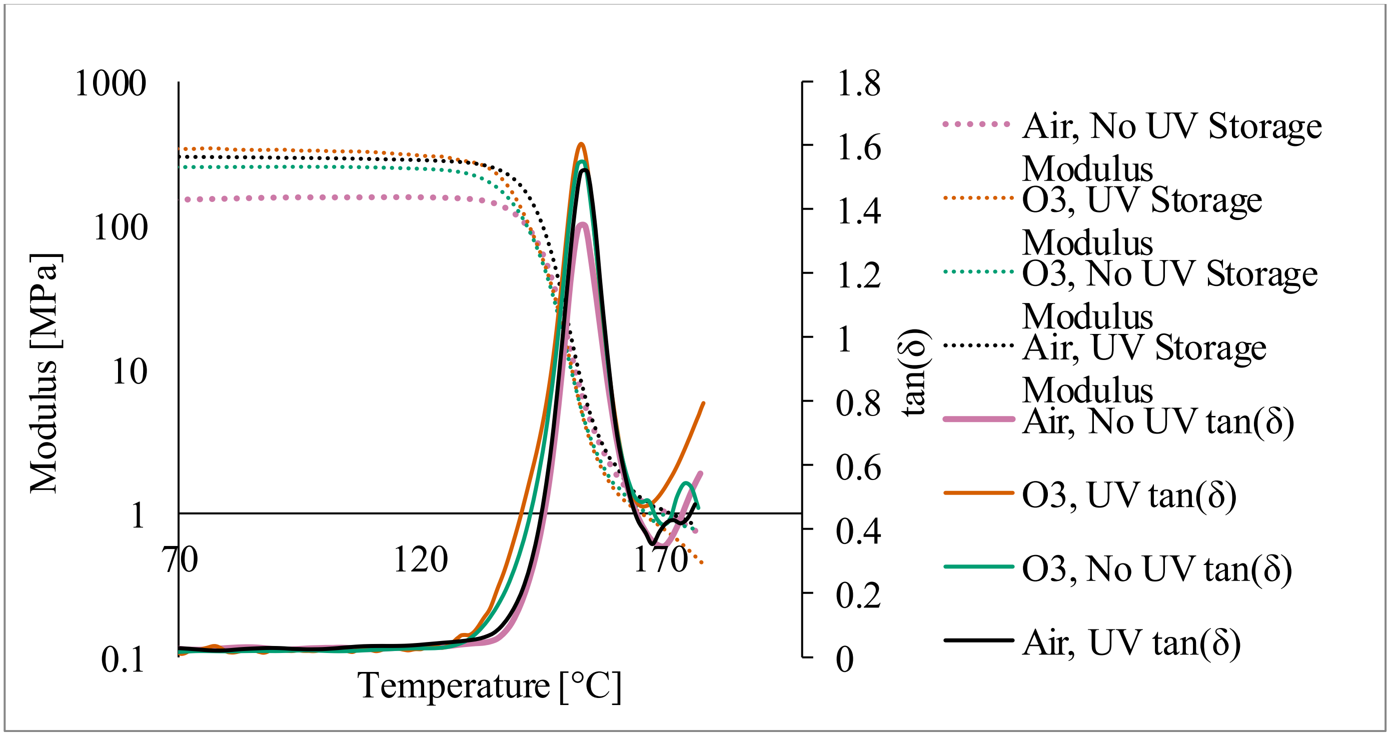

Figure 7: A graph showing tan(δ) (solid lines) and storage modulus (dashed lines). The sample exposed to ozone and UV light has the broadest peak base.

D. Differential Scanning Calorimetry (DSC)

The glass transition temperature from the DSC for the samples printed in air was found to be 139.9 °C, with a standard deviation of 1.0 °C. For the samples printed under UV light and an ozone atmosphere, the glass transition was found to be 140.7 °C, with a standard deviation of 0.4 °C. There is no statistically significant difference between the two because the standard deviations overlap. The DSC curves are plotted in Figure 8, showing cooling and the second heat of the DSC method. As polycarbonate is amorphous, there is no melting point seen with either condition. It was found that there was no significant change in the material visible by the DSC instrument. As the DSC is a weight-based technique, the consistency of the two curves implicates that little mass was affected.[13]

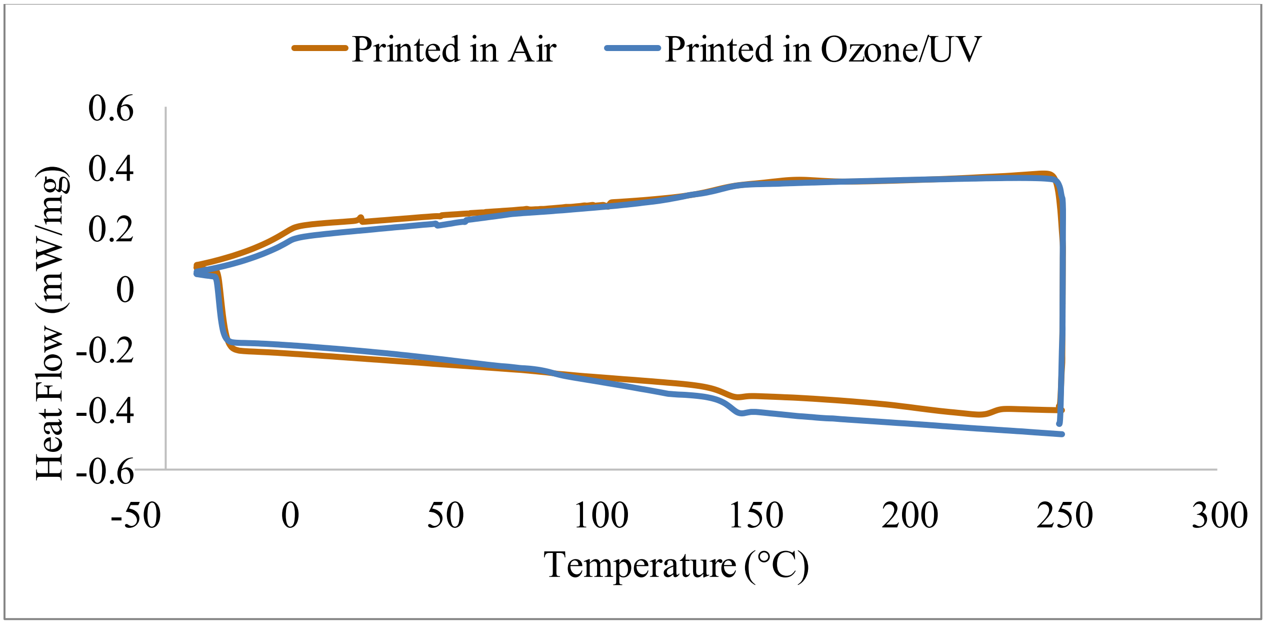

Figure 8: The graph shows the cool-heat procedure. No significant difference is seen between the treated and untreated samples.

IV. Future Work

This work demonstrated the idea that a bulk material change can be made by printing in a reactive gas. Further study will need to be made to determine what effect this process causes to the strength or durability of the part. Beyond this reaction with polycarbonate and ozone/UV light, other polymer gas reactions should be studied. A reactive gas can also be introduced during printing a polymer blend, leading to unique properties. This work demonstrated success of the concept, which can contribute to a catalog of different in situ gas modifications. These reactions can also be studied as they progress, and modeling should be done to understand the mechanics of each reaction. These studies will further the applications of additive manufacturing and increase the flexibility of this manufacturing method.

V. Conclusion

Polycarbonate was successfully printed via FFF in a reactive gas atmosphere, affecting each layer of the part to alter bulk properties. Evidence of chemical change was seen visually and on the surface with FTIR-ATR. The bulk chemical change manifested as tan(δ) peak broadening and a room temperature modulus increase measured through DMA. The change in bulk properties was done without the extra time or processing step needed if a liquid phase material was sprayed on each individual layer. This is important to show that it is possible to expand the scope of material properties achieved through FFF. This allows the agility to change properties with a single polymer material by changing the reactive gas atmosphere. With only a single material, a variety of properties can be developed, even across a single part. The benefits of FFF will have more applications as the capabilities of the manufacturing technique increases. Printing in a reactive atmosphere is an important step in expanding those capabilities. Understanding that it is possible to create bulk property changes without added time leads to future reactions and properties to be explored.

VI. Acknowledgments

This project was funded by Savannah River National Laboratory's (SRNL) Laboratory Directed Research and Development (LDRD) program through project #LDRD-2022-00016. S. B. Hall was supported through the DOE Office of Science through the Summer Undergraduate Laboratory Internship (SULI) program. The authors would like to thank Dr. Louis McNamara for his help in collecting FTIR data.

VII. References

1. C. A. Chatham, Arit Dasa, Jacob J. Fallona, Callie E. Zawaskia, Eric L. Gilmera, and M. J. B. Christopher B. Williamsa, Additive Manufacturing **34** (2020).
2. J. Mikeš, S. Pekárek, O. Babčenko, O. Hanuš, J. Kákona and P. Štenclová, Plasma Processes and Polymers **17** (1) (2019).
3. C. A. Chatham, C. E. Zawaski, D. C. Bobbitt, R. B. Moore, T. E. Long and C. B. Williams, Macromolecular Materials and Engineering **304** (5) (2019).
4. X. Gao, S. Qi, X. Kuang, Y. Su, J. Li and D. Wang, Additive Manufacturing **37** (2021).
5. D. Jiang and D. E. Smith, Additive Manufacturing **18**, 84-94 (2017).
6. S. C. Perryman and M. D. Dadmun, Additive Manufacturing **38** (2021).
7. W. Chen, K. G. NEOH, E. T. Kang, K. L. Tan, D. J. LIAW and C. C. HUANG, Journal of Polymer Science: Part A: Polymer Chemistry **36**, 357-386 (1998).
8. A. S. Bhurke, P. A. Askeland and L. T. Drzal, The Journal of Adhesion **83** (1), 43-66 (2007).
9. P. Urwyler, A. Pascual, B. Müller and H. Schift, Journal of Applied Polymer Science **132** (18), n/a-n/a (2015).
10. J. R. Vig, Journal of Vacuum Science & Technology A: Vacuum, Surfaces, and Films **3** (3), 1027-1034 (1985).
11. J. E. Seppala and K. D. Migler, Addit Manuf **12** (Pt A), 71-76 (2016).
12. R. O. F. Verkuijlen, M. H. A. van Dongen, A. A. E. Stevens, J. van Geldrop and J. P. C. Bernards, Applied Surface Science **290**, 381-387 (2014).
13. Y. Z. Qiuju Zheng, Maziar Montazerian, Ozgur Gulbiten, John C. Mauro, Edgar D. Zanotto, and Yuanzheng Yue, Chemical Reviews **119**, 7848−7939 (2019).
14. #3DBenchy. 2022. *#3DBenchy*. [online] Available at: <https://www.3dbenchy.com/> [Accessed 21 July 2022].

VIII. Appendix

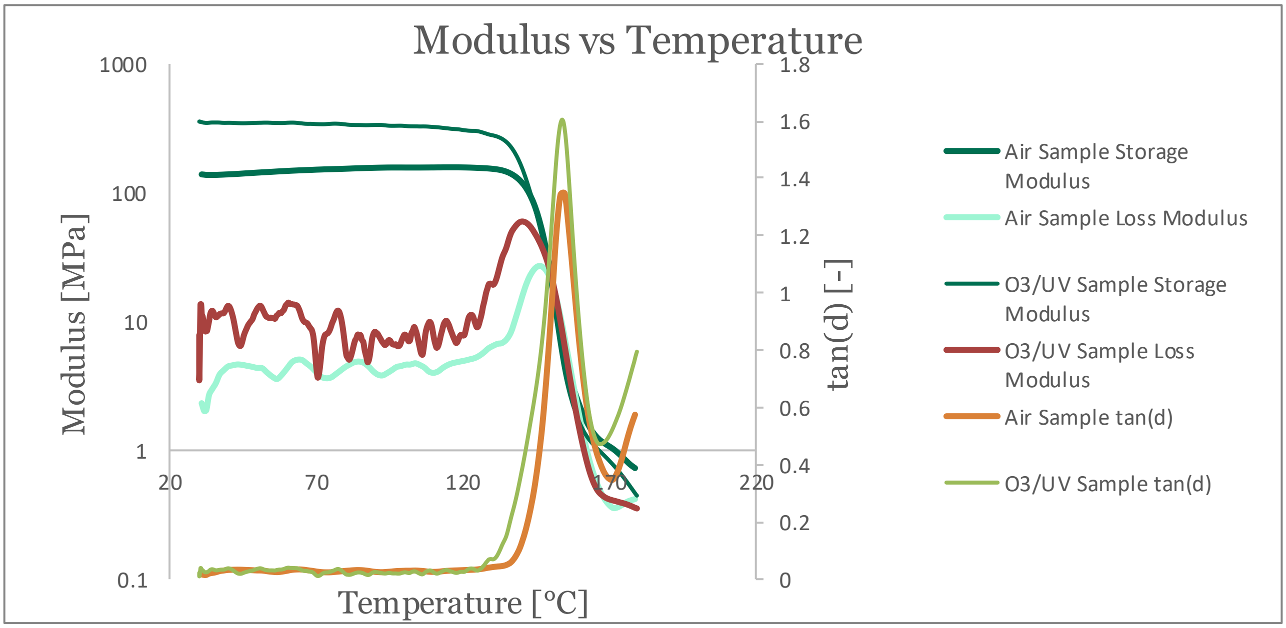

Fig 9: The full DMA graph including storage and loss modulus, and tan(δ).